Robust Power Allocation Algorithms for Wireless Relay Networks

Robust Power Allocation Algorithms for Wireless Relay Networks

Tony Q.S. Quek, *Member, IEEE,* Moe Z. Win, *Fellow, IEEE,* and Marco Chiani, *Senior Member, IEEE*

***Abstract*—Resource allocation promises significant benefits in wireless networks. In order to fully reap these benefits, it is important to design efficient resource allocation algorithms. Here, we develop relay power allocation (RPA) algorithms for coherent and noncoherent amplify-and-forward (AF) relay networks. The goal is to maximize the output signal-to-noise ratio under individual as well as aggregate relay power constraints. We show that these RPA problems, in the presence of perfect global channel state information (CSI), can be formulated as quasiconvex optimization problems. In such settings, the optimal solutions can be efficiently obtained via a sequence of convex feasibility problems, in the form of second-order cone programs. The benefits of our RPA algorithms, however, depend on the quality of the global CSI, which is rarely perfect in practice. To address this issue, we introduce the robust optimization methodology that accounts for uncertainties in the global CSI. We show that the robust counterparts of our convex feasibility problems with ellipsoidal uncertainty sets are semi-definite programs. Our results reveal that ignoring uncertainties associated with global CSI often leads to poor performance, highlighting the importance of robust algorithm designs in practical wireless networks.**

***Index Terms*—Relay networks, power allocation, amplify-and-forward relaying, robust optimization, semi-definite program.**

I. INTRODUCTION

RESOURCE allocation in wireless networks promises significant benefits such as higher throughput, longer network lifetime, and lower network interference. In relay networks, the primary resource is the transmission power because it affects both the lifetime and the scalability of the network. Furthermore, regulatory agencies may limit the total transmission power to reduce interference to other users. Some important questions then arise naturally in practice:

- How can we control network interference by incorporating individual relay and aggregate power constraints in our relay power allocation (RPA) algorithms?
- What are the fundamental limits on performance gains that can be achieved with RPA when uncertainties exist in the global channel state information (CSI)?
- Is it possible to design RPA algorithms that are robust to uncertainties in global CSI?

To address these issues of robustness, we adopt as in [1], a robust optimization methodology developed in [2], [3]. Specifically, this methodology treats uncertainty by assuming that CSI is a deterministic variable within a bounded set of possible values. The size of the uncertainty set corresponds to the amount of uncertainty on the CSI.[1] This methodology ensures that the robust counterpart of uncertain optimization problem, i.e., optimization problem with uncertain global CSI, leads to feasible solutions and yields good performance for all realizations of CSI within the uncertainty set.

Here, we focus on an amplify-and-forward (AF) relay network. In particular, we consider coherent and noncoherent AF relaying, depending on the knowledge of CSI available at each relay node. The AF relaying is attractive due to its simplicity, security, power-efficiency, and ability to realize full diversity order. Moreover, the AF relaying has been shown to be optimal in certain scenarios[4]. There are several works related to finding the optimal RPA under different conditions. For example, in [5], the asymptotically optimal power and rate allocation, as the channel bandwidth goes to infinity, for Gaussian AF relay channels under a total network power constraint is determined. In [6], the optimal RPA for a three-node network in high signal-to-noise ratio (SNR) regime is derived. The optimal RPA was derived for noncoherent AF relay channels under a total network power constraint in [7]. In [8], the optimal RPA for multihop noncoherent AF relay channels under both individual and total relay power constraints is derived. However, all the above works[5]–[8] assume that perfect global CSI is available. In practice, such an assumption is too optimistic since the knowledge of global CSI is rarely perfect in practice, i.e., uncertainties in CSI arise as a consequence of imperfect channel estimation, quantization, synchronization, hardware limitations, implementation errors, or transmission errors in feedback channels.[2] In general, imperfect CSI leads to performance degradation of wireless systems[10].

In this paper, we develop RPA algorithms for coherent and noncoherent AF relay networks[11], [12]. The problem formulation is such that the output SNR is maximized subject to *both* individual and aggregate relay power constraints. We show that the coherent AF RPA problem, in the presence of perfect global CSI, can be formulated as a quasiconvex optimization problem. This problem can be solved efficiently using the bisection method through a sequence of convex

Paper approved by G.-H. Im, the Editor for Equalization and Multicarrier Techniques of the IEEE Communications Society. Manuscript received June 10, 2008; revised April 27, 2009, July 31, 2009, and October 9, 2009.

T. Q.S. Quek is with the Institute for Infocomm Research, 1 Fusionopolis Way, #21-01 Connexis South Tower, Singapore 138632 (e-mail: qsquek@ieee.org).

M. Z. Win is with the Laboratory for Information & Decision Systems (LIDS), Massachusetts Institute of Technology, 77 Massachusetts Avenue, Cambridge, MA 02139 (e-mail: moewin@mit.edu).

M. Chiani is with DEIS, WiLAB, University of Bologna, Viale Risorgimento 2, 40136 Bologna, Italy (e-mail: marco.chiani@unibo.it).

This research was supported in part by the Office of Naval Research Young Investigator Award N00014-03-1-0489, the National Science Foundation under Grants ANI-0335256 and ECS-0636519, DOCOMO USA Labs, the Charles Stark Draper Laboratory Reduced Complexity UWB Communication Techniques Program, the Institute of Advanced Study Natural Science & Technology Fellowship, and the FP7 ICT project EUWB.

Digital Object Identifier 10.1109/TCOMM.2010.07.080277

[1]The singleton uncertainty set corresponds to the case of perfect CSI.

[2]Exactly how this global CSI can be obtained at the central network controller is beyond the scope of this paper. Some related work can be found in [9].

feasibility problems, which can be cast as second-order cone programs (SOCPs)[13]. We also show that the noncoherent AF RPA problem, in the presence of perfect global CSI, can be approximately decomposed into $2L$ quasiconvex optimization subproblems. Each subproblem can be solved efficiently by the bisection method via a sequence of convex feasibility problems in the form of SOCP. We then develop the robust optimization framework for RPA problems in the case of uncertain global CSI. We show that the robust counterparts of our convex feasibility problems with ellipsoidal uncertainty sets can be formulated as semi-definite programs (SDPs). Our results reveal that ignoring uncertainties associated with global CSI in RPA algorithms often leads to poor performance, highlighting the importance of robust algorithm designs in wireless networks.

The paper is organized as follows. In Section II, the problem formulation is described. In Section III, we formulate the coherent and noncoherent AF RPA problems as quasiconvex optimization problems. Next, in Section IV, we formulate the robust counterparts of our RPA problems when the global CSI is subject to uncertainty. Numerical results are presented in Section V and conclusions are given in the last section.

Notations: Throughout the paper, we shall use the following notation. Boldface upper-case letters denote matrices, boldface lower-case letters denote column vectors, and plain lower-case letters denote scalars. The superscripts $(\cdot)^T$, $(\cdot)^*$, and $(\cdot)^\dagger$ denote the transpose, complex conjugate, and transpose conjugate respectively. We denote a standard basis vector with a one at the kth element as $\boldsymbol{e}_k$, $n \times n$ identity matrix as $\boldsymbol{I}_n$, and (i, j)th element of $\boldsymbol{B}$ as $[\boldsymbol{B}]_{ij}$. The notations $\operatorname{tr}(\cdot)$, $|\cdot|$ and $\|\cdot\|$ denote the trace operator, absolute value and the standard Euclidean norm, respectively. We denote the nonnegative and positive orthants in Euclidean vector space of dimension K as $\mathbb{R}^K_+$ and $\mathbb{R}^K_{++}$, respectively. We denote $\boldsymbol{B} \succeq 0$ and $\boldsymbol{B} \succ 0$ as $\boldsymbol{B}$ being positive semi-definite and positive definite, respectively.

II. Problem Formulation

We consider a wireless relay network consisting of $N_\mathrm{r} + 2$ nodes, each with single-antenna: a designated source-destination node pair together with N_r relay nodes located randomly and independently in a fixed area. We consider a scenario in which there is no direct link between the source and destination nodes and all nodes are operating in a common frequency band.

Transmission occurs over two time slots. In the first time slot, the relay nodes receive the signal transmitted by the source node. After processing the received signals, the relay nodes transmit the processed data to the destination node during the second time slot while the source node remains silent. We assume perfect synchronization at the destination node.[3] The received signals at the relay and destination nodes can then be written as

$$\boldsymbol{y}_\mathrm{R} = \boldsymbol{h}_\mathrm{B} x_\mathrm{S} + \boldsymbol{z}_\mathrm{R}, \qquad \text{First slot} \tag{1}$$

$$y_\mathrm{D} = \boldsymbol{h}_\mathrm{F}^T \boldsymbol{x}_\mathrm{R} + z_\mathrm{D}, \qquad \text{Second slot} \tag{2}$$

where x_S is the transmitted signal from the source node to the relay nodes, $\boldsymbol{x}_\mathrm{R}$ is the $N_\mathrm{r} \times 1$ transmitted signal vector from the relay nodes to the destination node, $\boldsymbol{y}_\mathrm{R}$ is the $N_\mathrm{r} \times 1$ received signal vector at the relay nodes, y_D is the received signal at the destination node, $\boldsymbol{z}_\mathrm{R} \sim \tilde{\mathcal{N}}_{N_\mathrm{r}}(\boldsymbol{0}, \boldsymbol{\Sigma}_\mathrm{R})$ is the $N_\mathrm{r} \times 1$ noise vector at the relay nodes, and $z_\mathrm{D} \sim \tilde{\mathcal{N}}(0, \sigma_\mathrm{D}^2)$ is the noise at the destination node.[4] Note that the different noise variances at the relay nodes are reflected in $\boldsymbol{\Sigma}_\mathrm{R} \triangleq \operatorname{diag}(\sigma^2_{\mathrm{R},1}, \sigma^2_{\mathrm{R},2}, \ldots, \sigma^2_{\mathrm{R},N_\mathrm{r}})$. Moreover, $\boldsymbol{z}_\mathrm{R}$ and z_D are independent. Furthermore, they are mutually uncorrelated with x_S and $\boldsymbol{x}_\mathrm{R}$. With perfect global CSI at the destination node, $\boldsymbol{h}_\mathrm{B}$ and $\boldsymbol{h}_\mathrm{F}$ are $N_\mathrm{r} \times 1$ known channel vectors from source to relay and from relay to destination, respectively, where $\boldsymbol{h}_\mathrm{B} = [h_{\mathrm{B},1}, h_{\mathrm{B},2}, \ldots, h_{\mathrm{B},N_\mathrm{r}}]^T \in \mathbb{C}^{N_\mathrm{r}}$ and $\boldsymbol{h}_\mathrm{F} = [h_{\mathrm{F},1}, h_{\mathrm{F},2}, \ldots, h_{\mathrm{F},N_\mathrm{r}}]^T \in \mathbb{C}^{N_\mathrm{r}}$. For convenience, we shall refer to $\boldsymbol{h}_\mathrm{B}$ as the backward channel and $\boldsymbol{h}_\mathrm{F}$ as the forward channel.

At the source node, we impose an individual source power constraint P_S, such that $\mathbb{E}\{|x_\mathrm{S}|^2\} \leq P_\mathrm{S}$. Similarly, at the relay nodes, we impose both individual relay power constraint P and aggregate relay power constraint P_R such that the transmission power allocated to the kth relay node $p_k \triangleq [\boldsymbol{Q}_\mathrm{R}]_{k,k} \leq P$ for $k \in \mathcal{N}_\mathrm{r}$ and $\operatorname{tr}(\boldsymbol{Q}_\mathrm{R}) \leq P_\mathrm{R}$, where $\boldsymbol{Q}_\mathrm{R} \triangleq \mathbb{E}\{\boldsymbol{x}_\mathrm{R}\boldsymbol{x}_\mathrm{R}^\dagger |\, \boldsymbol{h}_\mathrm{B}\}$ and $\mathcal{N}_\mathrm{r} = \{1, 2, \ldots, N_\mathrm{r}\}$.

For AF relaying, the relay nodes simply transmit scaled versions of their received signals while satisfying power constraints. In this case, $\boldsymbol{x}_\mathrm{R}$ in (2) is given by

$$\boldsymbol{x}_\mathrm{R} = \boldsymbol{G}\boldsymbol{y}_\mathrm{R} \tag{3}$$

where $\boldsymbol{G}$ denotes the $N_\mathrm{r} \times N_\mathrm{r}$ diagonal matrix representing relay gains and thus[5]

$$\boldsymbol{Q}_\mathrm{R} = \boldsymbol{G}\left(P_\mathrm{S}\boldsymbol{h}_\mathrm{B}\boldsymbol{h}_\mathrm{B}^\dagger + \boldsymbol{\Sigma}_\mathrm{R}\right)\boldsymbol{G}^\dagger. \tag{4}$$

The diagonal structure of $\boldsymbol{G}$ ensures that each relay node only requires the knowledge about its own received signal. When each relay node has access to its locally-bidirectional CSI, it can perform distributed beamforming.[6] As such, this is referred to as coherent AF relaying and the kth diagonal element of $\boldsymbol{G}$ is given by[4]

$$g_\mathrm{coh}^{(k)} = \sqrt{\beta_k p_k}\,\frac{h^*_{\mathrm{B},k}}{|h_{\mathrm{B},k}|}\,\frac{h^*_{\mathrm{F},k}}{|h_{\mathrm{F},k}|} \tag{5}$$

where $\beta_k = 1/(P_\mathrm{S}|h_{\mathrm{B},k}|^2 + \sigma^2_{\mathrm{R},k})$. On the other hand, when forward CSI is absent at each relay node, the relay node simply forwards a scaled version of its received signal without any phase alignment. This is referred to as noncoherent AF relaying and the kth diagonal element of $\boldsymbol{G}$ is given by[7], [8]

$$g_\mathrm{noncoh}^{(k)} = \sqrt{\beta_k p_k}. \tag{6}$$

[3]Exactly how to achieve this synchronization or the effect of small synchronization errors on performance is beyond the scope of this paper.

[4]$\tilde{\mathcal{N}}(\mu, \sigma_2)$ denotes a complex circularly symmetric Gaussian distribution with mean μ and variance σ^2. Similarly, $\tilde{\mathcal{N}}_K(\boldsymbol{\mu}, \boldsymbol{\Sigma})$ denotes a complex K-variate Gaussian distribution with a mean vector $\boldsymbol{\mu}$ and a covariance matrix $\boldsymbol{\Sigma}$.

[5]Note that in (4), the source employs the maximum allowable power P_S in order to maximize the SNR at the destination node.

[6]Here, locally-bidirectional CSI refers to the knowledge of only $h_{\mathrm{B},k}$ and $h_{\mathrm{F},k}$ at the kth relay node.

It follows from (1)-(3) that the received signal at the destination node can be written as

$$y_{\rm D} = \boldsymbol{h}_{\rm F}^T \boldsymbol{G} \boldsymbol{h}_{\rm B} x_{\rm S} + \underbrace{\boldsymbol{h}_{\rm F}^T \boldsymbol{G} \boldsymbol{z}_{\rm R} + z_{\rm D}}_{\triangleq \tilde{z}_{\rm D}} \tag{7}$$

where $\tilde{z}_{\rm D}$ represents the effective noise at the destination node, and the instantaneous SNR at the destination node conditioned on $\boldsymbol{h}_{\rm B}$ and $\boldsymbol{h}_{\rm F}$ is then given by

$$\begin{aligned}\mathsf{SNR}(\boldsymbol{p}) &\triangleq \frac{\mathbb{E}\left\{|\boldsymbol{h}_{\rm F}^T \boldsymbol{G} \boldsymbol{h}_{\rm B} x_{\rm S}|^2 \,|\boldsymbol{h}_{\rm B}, \boldsymbol{h}_{\rm F}\right\}}{\mathbb{E}\left\{|\tilde{z}_{\rm D}|^2 \,|\boldsymbol{h}_{\rm F}\right\}} \\ &= \frac{P_{\rm S} \boldsymbol{h}_{\rm F}^T \boldsymbol{G} \boldsymbol{h}_{\rm B} \boldsymbol{h}_{\rm B}^\dagger \boldsymbol{G}^\dagger \boldsymbol{h}_{\rm F}^*}{\boldsymbol{h}_{\rm F}^T \boldsymbol{G} \boldsymbol{\Sigma}_{\rm R} \boldsymbol{G}^\dagger \boldsymbol{h}_{\rm F}^* + \sigma_{\rm D}^2}\end{aligned} \tag{8}$$

where $\boldsymbol{p} = [p_1, p_2, \ldots, p_{N_{\rm r}}]^T$. Our goal is to maximize system performance by optimally allocating transmission power of the relay nodes. We adopt the SNR at the destination node as the performance metric and formulate the RPA problem as follows:

$$\begin{array}{ll} \max\limits_{\boldsymbol{p}} & \mathsf{SNR}(\boldsymbol{p}) \\ \text{s.t.} & \operatorname{tr}(\boldsymbol{Q}_{\rm R}) \leq P_{\rm R}, \\ & 0 \leq [\boldsymbol{Q}_{\rm R}]_{k,k} \leq P, \quad \forall k \in \mathcal{N}_{\rm r}. \end{array} \tag{9}$$

Note that the optimal solution to the problem in (9) maximizes the capacity of the AF relay network under perfect global CSI since this capacity, given by $\frac{1}{2}\log(1 + \mathsf{SNR})$, is a monotonically increasing function of SNR.

III. Optimal Relay Power Allocation

A. Coherent AF Relaying

First, we transform (9) for the coherent AF RPA problem into a quasiconvex optimization problem as given in the following proposition.

Proposition 1: The coherent AF relay power allocation problem can be transformed into a quasiconvex optimization problem as

$$\begin{array}{ll} \mathcal{P}_{\rm coh} : \max\limits_{\boldsymbol{\zeta}} & f_{\rm coh}(\boldsymbol{\zeta}) \triangleq \frac{P_{\rm S}}{\sigma_{\rm D}^2} \frac{(\boldsymbol{c}^T \boldsymbol{\zeta})^2}{\|\boldsymbol{A}\boldsymbol{\zeta}\|^2 + 1} \\ \qquad\text{s.t.} & \boldsymbol{\zeta} \in \mathcal{S} \end{array} \tag{10}$$

and the feasible set $\mathcal{S}$ is given by

$$\mathcal{S} = \left\{ \boldsymbol{\zeta} \in \mathbb{R}_+^{N_{\rm r}} : \sum_{k \in \mathcal{N}_{\rm r}} \zeta_k^2 \leq 1, \; 0 \leq \zeta_k \leq \sqrt{\eta_{\rm p}}, \; \forall k \in \mathcal{N}_{\rm r} \right\}$$

where $\zeta_k \triangleq \sqrt{\frac{p_k}{P_{\rm R}}}$ is the optimization variable and $\eta_{\rm p} \triangleq P/P_{\rm R}$. In addition, $\boldsymbol{c} = [c_1, c_2, \ldots, c_{N_{\rm r}}]^T \in \mathbb{R}_+^{N_{\rm r}}$, and $\boldsymbol{A} = \operatorname{diag}(a_1, a_2, \ldots, a_{N_{\rm r}}) \in \mathbb{R}_+^{N_{\rm r} \times N_{\rm r}}$ are defined for notational convenience where

$$c_k = \sqrt{\beta_k P_{\rm R}}\; |h_{{\rm B},k}||h_{{\rm F},k}| \tag{11}$$

$$a_k = \frac{\sqrt{\beta_k P_{\rm R}}\; |h_{{\rm F},k}| \sigma_{{\rm R},k}}{\sigma_{\rm D}}. \tag{12}$$

Proof: See Appendix A. □

Remark 1: Note that ζ_k denotes the fractional power allocated to the kth relay node, and $\eta_{\rm p}$ denotes the ratio between the individual relay power constraint and the aggregate relay power constraint, where $0 < \eta_{\rm p} \leq 1$. It is well-known that we can solve $\mathcal{P}_{\rm coh}$ efficiently through a sequence of convex feasibility problems using the bisection method[14]. In our case, we can always let $t_{\min}$ corresponding to the uniform RPA and we only need to choose $t_{\max}$ appropriately. We formalize these results in the following algorithm.

Algorithm 1: The program $\mathcal{P}_{\rm coh}$ in Proposition 1 can be solved numerically using the bisection method:

0. *Initialize $t_{\min} = f_{\rm coh}(\boldsymbol{\zeta}_{\min})$, $t_{\max} = f_{\rm coh}(\boldsymbol{\zeta}_{\max})$, where $f_{\rm coh}(\boldsymbol{\zeta}_{\min})$ and $f_{\rm coh}(\boldsymbol{\zeta}_{\max})$ define a range of relevant values of $f_{\rm coh}(\boldsymbol{\zeta})$, and set tolerance $\varepsilon \in \mathbb{R}_{++}$.*
1. *Solve the convex feasibility program $\mathcal{P}_{\rm coh}^{\rm (SOCP)}(t)$ in (13) by fixing $t = (t_{\max} + t_{\min})/2$.*
2. *If $\mathcal{S}_{\rm coh}(t) = \emptyset$, then set $t_{\max} = t$ else set $t_{\min} = t$.*
3. *Stop if the gap $(t_{\max} - t_{\min})$ is less than the tolerance ε. Go to Step 1 otherwise.*
4. *Output $\boldsymbol{\zeta}_{\rm opt}$ obtained from solving $\mathcal{P}_{\rm coh}^{\rm (SOCP)}(t)$ in Step 1.*

where the convex feasibility program can be written in SOCP form as

$$\begin{array}{ll} \mathcal{P}_{\rm coh}^{\rm (SOCP)}(t) : \text{find} & \boldsymbol{\zeta} \\ \qquad\qquad\text{s.t.} & \boldsymbol{\zeta} \in \mathcal{S}_{\rm coh}(t) \end{array} \tag{13}$$

with the set $\mathcal{S}_{\rm coh}(t)$ given by

$$\begin{aligned}\mathcal{S}_{\rm coh}(t) = \Bigg\{ \boldsymbol{\zeta} \in \mathbb{R}_+^{N_{\rm r}} : & \begin{bmatrix} \boldsymbol{c}^T \boldsymbol{\zeta} \sqrt{\frac{P_{\rm S}}{t\sigma_{\rm D}^2}} \\ \begin{pmatrix} 1 \\ \boldsymbol{A}\boldsymbol{\zeta} \end{pmatrix} \end{bmatrix} \succeq_{\mathcal{K}} 0, \; \begin{bmatrix} 1 \\ \boldsymbol{\zeta} \end{bmatrix} \succeq_{\mathcal{K}} 0, \\ & \begin{bmatrix} \frac{\eta_{\rm p}+1}{2} \\ \begin{pmatrix} \boldsymbol{\zeta}^T \boldsymbol{e}_k \\ \frac{\eta_{\rm p}-1}{2} \end{pmatrix} \end{bmatrix} \succeq_{\mathcal{K}} 0, \quad \forall k \in \mathcal{N}_{\rm r} \Bigg\}.\end{aligned} \tag{14}$$

Proof: See Appendix B. □

B. Noncoherent AF Relaying

Similar to the formulation of coherent AF RPA problem in (10), we can expressed the noncoherent AF RPA problem as

$$\begin{array}{ll} \mathcal{P}_{\rm noncoh} : \max\limits_{\boldsymbol{\zeta}} & \frac{P_{\rm S}}{\sigma_{\rm D}^2} \frac{|\boldsymbol{c}^T \boldsymbol{\zeta}|^2}{\|\boldsymbol{A}\boldsymbol{\zeta}\|^2 + 1} \\ \qquad\text{s.t.} & \boldsymbol{\zeta} \in \mathcal{S} \end{array} \tag{15}$$

where $\mathcal{S}$ and $\boldsymbol{A}$ are given in Proposition 1. The difference is in $\boldsymbol{c} = [c_1, c_2, \ldots, c_{N_{\rm r}}] \in \mathbb{C}^{N_{\rm r}}$, where

$$c_k = \sqrt{\beta_k P_{\rm R}}\; h_{{\rm B},k} h_{{\rm F},k}.$$

As a result, we cannot directly apply Algorithm 1 to solve $\mathcal{P}_{\rm noncoh}$ in (15). Instead, we introduce the following lemma which enables us to decompose $\mathcal{P}_{\rm noncoh}$ into $2L$ quasiconvex optimization subproblems, each of which can then be solved efficiently via the algorithm presented in Algorithm 1.

Lemma 1 (Linear Approximation of Modulus[15]): The modulus of a complex number $Z \in \mathbb{C}$ can be linearly approximated with the polyhedral norm given by

$$p_L(Z) = \max_{l \in \mathcal{L}} \left\{ \mathfrak{Re}\{Z\} \cos\left(\frac{l\pi}{L}\right) + \mathfrak{Im}\{Z\} \sin\left(\frac{l\pi}{L}\right) \right\}$$

where $\mathcal{L} = \{1, 2, \ldots, 2L\}$, $\mathfrak{Re}\{Z\}$ *and* $\mathfrak{Im}\{Z\}$ *denote the real and imaginary parts of* Z*, and the polyhedral norm* $p_L(Z)$ *is bounded by*

$$p_L(Z) \le |Z| \le p_L(Z) \sec\left(\frac{\pi}{2L}\right).$$

and L is a positive integer such that $L \ge 2$.

Proposition 2: The noncoherent AF relay power allocation problem can be approximately decomposed into $2L$ *quasiconvex optimization subproblems. The master problem can be written as*

$$\max_{l \in \mathcal{L}} \quad f_{\text{noncoh}}(\boldsymbol{\zeta}_l^{\text{opt}}) \tag{16}$$

where

$$f_{\text{noncoh}}(\boldsymbol{\zeta}) \triangleq \frac{P_{\text{S}}}{\sigma_{\text{D}}^2} \frac{\left[\mathfrak{Re}\left\{\boldsymbol{c}^T\boldsymbol{\zeta}\right\}\cos(l\pi/L) + \mathfrak{Im}\left\{\boldsymbol{c}^T\boldsymbol{\zeta}\right\}\sin(l\pi/L)\right]^2}{\|\boldsymbol{A}\boldsymbol{\zeta}\|^2 + 1}$$

and $\boldsymbol{\zeta}_l^{\text{opt}}$ *is the optimal solution of the following subproblem*:

$$\begin{array}{lll} \mathcal{P}_{\text{noncoh}}(l) : \max\limits_{\boldsymbol{\zeta}_l} & f_{\text{noncoh}}(\boldsymbol{\zeta}_l) & \\ \quad\text{s.t.} & \mathfrak{Re}\left\{\boldsymbol{c}^T\boldsymbol{\zeta}_l\right\}\cos(l\pi/L) & \\ & +\mathfrak{Im}\left\{\boldsymbol{c}^T\boldsymbol{\zeta}_l\right\}\sin(l\pi/L) \ \ge \ 0, & \\ & \boldsymbol{\zeta}_l \in \mathcal{S}. & \end{array} \tag{17}$$

The feasible set $\mathcal{S}$ *is given by*

$$\mathcal{S} = \left\{ \boldsymbol{\zeta} \in \mathbb{R}_+^{N_{\text{r}}} : \sum_{k \in \mathcal{N}_{\text{r}}} \zeta_k^2 \le 1, \ 0 \le \zeta_k \le \sqrt{\eta_{\text{p}}}, \ \forall k \in \mathcal{N}_{\text{r}} \right\}$$

where $\zeta_k \triangleq \sqrt{\frac{p_k}{P_{\text{R}}}}$ *is the optimization variable and* $\eta_{\text{p}} \triangleq P/P_{\text{R}}$*. In addition,* $\boldsymbol{c} = [c_1, c_2, \ldots, c_{N_{\text{r}}}]^T \in \mathbb{C}^{N_{\text{r}}}$*, and* $\boldsymbol{A} = \text{diag}(a_1, a_2, \ldots, a_{N_{\text{r}}}) \in \mathbb{R}_+^{N_{\text{r}} \times N_{\text{r}}}$ *are defined as*

$$c_k = \sqrt{\beta_k P_{\text{R}}}\ h_{\text{B},k} h_{\text{F},k} \tag{18}$$

$$a_k = \frac{\sqrt{\beta_k P_{\text{R}}}\ |h_{\text{F},k}| \sigma_{\text{R},k}}{\sigma_{\text{D}}}. \tag{19}$$

Proof: Similar to the proof of Proposition 1. □

Remark 2: Note that $\mathcal{S}$ and $\boldsymbol{A}$ in Proposition 2 are exactly the same as that in Proposition 1. The difference is in $\boldsymbol{c}$ only. Unlike $\mathcal{P}_{\text{coh}}$, we now need to solve $2L$ quasiconvex optimization subproblems due to the approximation of $|\boldsymbol{c}^T\boldsymbol{\zeta}|$ using Lemma 1.

Algorithm 2: Each of the $2L$ *subproblems* $\mathcal{P}_{\text{noncoh}}(l)$ *in Proposition 2 can be solved efficiently by the bisection method via a sequence of convex feasibility problems in the form of SOCP. The* $2L$ *solutions* $\{\boldsymbol{\zeta}_l^{\text{opt}}\}_{l=1}^{2L}$ *then forms a candidate set for the optimal* $\boldsymbol{\zeta}^{\text{opt}}$ *that maximizes our master problem.*

Proof: The proof follows straightforwardly from Algorithm 1. □

IV. Robust Relay Power Allocation

A. Coherent AF Relaying

Using the above methodology, we formulate the robust counterpart of our AF RPA problem in Proposition 1 with uncertainties in $\boldsymbol{A}$ and $\boldsymbol{c}$, as follows:

$$\begin{array}{ll} \max\limits_{\boldsymbol{\zeta}} & f_{\text{coh}}(\boldsymbol{\zeta}, \boldsymbol{A}, \boldsymbol{c}) \\ \text{s.t.} & \boldsymbol{\zeta} \in \mathcal{S}, \quad \forall\,(\boldsymbol{A}, \boldsymbol{c}) \in \mathcal{U} \end{array} \tag{20}$$

where the feasible set $\mathcal{S}$ is given in Proposition 1 and $\mathcal{U}$ is an uncertainty set that contains all possible realizations of $\boldsymbol{A}$ and $\boldsymbol{c}$. To solve for the above optimization problem, we incorporate the uncertainties associated with $\boldsymbol{A}$ and $\boldsymbol{c}$ into the convex feasibility program in (13) of Algorithm 1. Since $(\boldsymbol{A}, \boldsymbol{c})$ only appears in the first constraint of (14), we simply need to focus on this constraint and build its robust counterpart as follows:

$$\boldsymbol{c}^T\boldsymbol{\zeta} \ge \sqrt{\frac{t\sigma_{\text{D}}^2}{P_{\text{S}}}(1 + \|\boldsymbol{A}\boldsymbol{\zeta}\|^2)}, \qquad \forall(\boldsymbol{A}, \boldsymbol{c}) \in \mathcal{U}. \tag{21}$$

In the following, we adopt a conservative approach which assumes that $\mathcal{U}$ affecting (21) is sidewise, i.e., the uncertainty affecting the right-hand side in (21) is independent of that affecting the left-hand side. Specifically, we have $\mathcal{U} = \mathcal{U}_{\text{R}} \times \mathcal{U}_{\text{L}}$. Without such an assumption, it is known that a computationally tractable robust counterpart for (21) does not exist, which makes the conservative approach rather attractive[2]. Our results are summarized in the next theorem.

Theorem 1: The robust coherent AF relay power allocation problem in (20) can be solved numerically via Algorithm 1, except that the convex feasibility program is now conservatively replaced by its robust counterpart given as follows:

$$\begin{array}{lll} \mathcal{P}_{\text{coh}}^{(\text{robust})}(t) : \text{find} & \boldsymbol{\zeta} \\ \quad\text{s.t.} & \boldsymbol{\zeta} \in \mathcal{S}_{\text{coh}}(t, \boldsymbol{A}, \boldsymbol{c}), \forall \boldsymbol{A} \in \mathcal{U}_{\text{R}}, \boldsymbol{c} \in \mathcal{U}_{\text{L}} \end{array} \tag{22}$$

with the sidewise independent ellipsoidal uncertainty sets $\mathcal{U}_{\text{R}}$ *and* $\mathcal{U}_{\text{L}}$ *given by*

$$\mathcal{U}_{\text{R}} = \left\{ \boldsymbol{A} = \boldsymbol{A}_0 + \sum_{j \in \mathcal{N}_A} z_j \boldsymbol{A}_j : \|\boldsymbol{z}\| \le \rho_1 \right\} \tag{23}$$

$$\mathcal{U}_{\text{L}} = \left\{ \boldsymbol{c} = \boldsymbol{c}_0 + \sum_{j \in \mathcal{N}_c} u_j \boldsymbol{c}_j : \|\boldsymbol{u}\| \le \rho_2 \right\} \tag{24}$$

where $\mathcal{N}_A = \{1, 2, \ldots, N_A\}$*,* $\mathcal{N}_c = \{1, 2, \ldots, N_c\}$*, and* N_A *and* N_c *are the dimensions of* $\boldsymbol{z}$ *and* $\boldsymbol{u}$*, respectively. Then, the approximate robust convex feasibility program* $\mathcal{P}_{\text{coh}}^{(\text{robust})}(t)$ *can be written in SDP form as:*

$$\begin{array}{ll} \text{find} & (\boldsymbol{\zeta}, \tau, \mu) \\ \text{s.t.} & (\boldsymbol{\zeta}, \tau, \mu) \in \mathcal{W}_{\text{coh}}(t) \end{array} \tag{25}$$

such that $(\boldsymbol{\zeta}, \tau, \mu) \in \mathbb{R}_+^{N_{\text{r}}} \times \mathbb{R}_+ \times \mathbb{R}_+$ *and the feasible set* $\mathcal{W}_{\text{coh}}(t)$ *is shown at the top of this page, where* $\breve{\boldsymbol{A}} = [\boldsymbol{A}_1\boldsymbol{\zeta}, \boldsymbol{A}_2\boldsymbol{\zeta}, \ldots, \boldsymbol{A}_{N_A}\boldsymbol{\zeta}]$ *and* $\breve{\boldsymbol{c}} = \left[\boldsymbol{c}_1^T\boldsymbol{\zeta}, \boldsymbol{c}_2^T\boldsymbol{\zeta}, \ldots, \boldsymbol{c}_{N_c}^T\boldsymbol{\zeta}\right]^T$.

Proof: The proof follows similar steps as in the proof of Theorem 6 in [1]. □

B. Noncoherent AF Relaying

In the next theorem, we formulate the robust counterparts of the $2L$ subproblems in Algorithm 2 with uncertainties associated with $\boldsymbol{A}$ and $\boldsymbol{c}$.

Theorem 2: The robust noncoherent AF relay power allocation problem can be approximately decomposed into $2L$ *subproblems. Under sidewise independent ellipsoidal uncertainty*

$$\mathcal{W}_{\mathrm{coh}}(t)=\left\{\boldsymbol{\zeta}\in\mathbb{R}_+^{N_\mathrm{r}}:\begin{bmatrix}\mu\boldsymbol{I}_{N_A} & \boldsymbol{0}_{N_A} & \breve{\boldsymbol{A}}^T\\ \boldsymbol{0}_{N_A}^T & \tau\sqrt{\frac{P_\mathrm{S}}{t\sigma_\mathrm{D}^2}}-\mu\rho_1^2-1 & \boldsymbol{\zeta}^T\boldsymbol{A}_0^T\\ \breve{\boldsymbol{A}} & \boldsymbol{A}_0\boldsymbol{\zeta} & \left(\tau\sqrt{\frac{P_\mathrm{S}}{t\sigma_\mathrm{D}^2}}-1\right)\boldsymbol{I}_{N_\mathrm{r}}\end{bmatrix}\succeq 0,\ \begin{bmatrix}\frac{(\boldsymbol{c}_0^T\boldsymbol{\zeta}-\tau)}{\rho_2}\boldsymbol{I}_{N_c} & \breve{\boldsymbol{c}}\\ \breve{\boldsymbol{c}}^T & \frac{(\boldsymbol{c}_0^T\boldsymbol{\zeta}-\tau)}{\rho_2}\end{bmatrix}\succeq 0,\right.$$
$$\left.\begin{bmatrix}\frac{\eta_\mathrm{P}+1}{2}\boldsymbol{I}_2 & \begin{pmatrix}\boldsymbol{\zeta}^T\boldsymbol{e}_k\\ \frac{\eta_\mathrm{P}-1}{2}\end{pmatrix}\\ \begin{pmatrix}\boldsymbol{\zeta}^T\boldsymbol{e}_k\\ \frac{\eta_\mathrm{P}-1}{2}\end{pmatrix}^T & \frac{\eta_\mathrm{P}+1}{2}\end{bmatrix}\succeq 0,\ \begin{bmatrix}\boldsymbol{I}_{N_\mathrm{r}} & \boldsymbol{\zeta}\\ \boldsymbol{\zeta}^T & 1\end{bmatrix}\succeq 0,\ \begin{bmatrix}\tau & \sqrt{\frac{t\sigma_\mathrm{D}^2}{P_\mathrm{S}}}\\ \sqrt{\frac{t\sigma_\mathrm{D}^2}{P_\mathrm{S}}} & \tau\end{bmatrix}\succeq 0,\quad \forall k\in\mathcal{N}_\mathrm{r}\right\}$$

$$\mathcal{W}_{\mathrm{noncoh}}(t,l)=\left\{\boldsymbol{\zeta}_l\in\mathbb{R}_+^{N_\mathrm{r}}:\begin{bmatrix}\mu\boldsymbol{I}_{N_A} & \boldsymbol{0}_{N_A} & \breve{\boldsymbol{A}}_l^T\\ \boldsymbol{0}_{N_A}^T & \tau\sqrt{\frac{P_\mathrm{S}}{t\sigma_\mathrm{D}^2}}-\mu\rho_1^2-1 & \boldsymbol{\zeta}_l^T\boldsymbol{A}_0^T\\ \breve{\boldsymbol{A}}_l & \boldsymbol{A}_0\boldsymbol{\zeta}_l & \left(\tau\sqrt{\frac{P_\mathrm{S}}{t\sigma_\mathrm{D}^2}}-1\right)\boldsymbol{I}_{N_\mathrm{r}}\end{bmatrix}\succeq 0,\ \begin{bmatrix}\frac{M(l)}{\rho_2}\boldsymbol{I}_{N_c} & \breve{\boldsymbol{c}}_l\\ \breve{\boldsymbol{c}}_l^T & \frac{M(l)}{\rho_2}\end{bmatrix}\succeq 0,\right.$$
$$\begin{bmatrix}\frac{\left[\mathfrak{Re}\left\{\boldsymbol{c}_0^T\boldsymbol{\zeta}_l\right\}\cos(l\pi/L)+\mathfrak{Im}\left\{\boldsymbol{c}_0^T\boldsymbol{\zeta}_l\right\}\sin(l\pi/L)\right]}{\rho_2}\boldsymbol{I}_{N_c} & \breve{\boldsymbol{c}}_l\\ \breve{\boldsymbol{c}}_l^T & \frac{\left[\mathfrak{Re}\left\{\boldsymbol{c}_0^T\boldsymbol{\zeta}_l\right\}\cos(l\pi/L)+\mathfrak{Im}\left\{\boldsymbol{c}_0^T\boldsymbol{\zeta}_l\right\}\sin(l\pi/L)\right]}{\rho_2}\end{bmatrix}\succeq 0,$$
$$\left.\begin{bmatrix}\frac{\eta_\mathrm{P}+1}{2}\boldsymbol{I}_2 & \begin{pmatrix}\boldsymbol{\zeta}_l^T\boldsymbol{e}_k\\ \frac{\eta_\mathrm{P}-1}{2}\end{pmatrix}\\ \begin{pmatrix}\boldsymbol{\zeta}_l^T\boldsymbol{e}_k\\ \frac{\eta_\mathrm{P}-1}{2}\end{pmatrix}^T & \frac{\eta_\mathrm{P}+1}{2}\end{bmatrix}\succeq 0,\ \begin{bmatrix}\boldsymbol{I}_{N_\mathrm{r}} & \boldsymbol{\zeta}_l\\ \boldsymbol{\zeta}_l^T & 1\end{bmatrix}\succeq 0,\ \begin{bmatrix}\tau & \sqrt{\frac{t\sigma_\mathrm{D}^2}{P_\mathrm{S}}}\\ \sqrt{\frac{t\sigma_\mathrm{D}^2}{P_\mathrm{S}}} & \tau\end{bmatrix}\succeq 0,\quad \forall k\in\mathcal{N}_\mathrm{r}\right\}$$

sets $\mathcal{U}_\mathrm{R}$ and $\mathcal{U}_\mathrm{L}$ given by

$$\mathcal{U}_\mathrm{R}=\left\{\boldsymbol{A}=\boldsymbol{A}_0+\sum_{j\in\mathcal{N}_A}z_j\boldsymbol{A}_j:\|\boldsymbol{z}\|\le\rho_1\right\},\qquad(26)$$

$$\mathcal{U}_\mathrm{L}=\left\{\boldsymbol{c}=\boldsymbol{c}_0+\sum_{j\in\mathcal{N}_c}u_j\boldsymbol{c}_j:\|\boldsymbol{u}\|\le\rho_2\right\}\qquad(27)$$

each subproblem can be solved efficiently using the bisection method, except that the convex feasibility program is now replaced with its approximate robust counterpart in the form of a SDP:

$$\begin{aligned}\mathcal{P}_{\mathrm{noncoh}}^{(\mathrm{robust})}(t,l):\ &\text{find} && (\boldsymbol{\zeta}_l,\tau,\mu)\\ &\text{s.t.} && (\boldsymbol{\zeta}_l,\tau,\mu)\in\mathcal{W}_{\mathrm{noncoh}}(t,l)\end{aligned}\qquad(28)$$

such that for each $l\in\mathcal{L}$, $(\boldsymbol{\zeta},\tau,\mu)\in\mathbb{R}_+^{N_\mathrm{r}}\times\mathbb{R}_+\times\mathbb{R}_+$, and the set $\mathcal{W}_{\mathrm{noncoh}}(t,l)$ is shown at the top of this page, where

$$\breve{\boldsymbol{c}}_l=\begin{bmatrix}\mathfrak{Re}\left\{\boldsymbol{c}_1^T\boldsymbol{\zeta}_l\right\}\cos(l\pi/L)+\mathfrak{Im}\left\{\boldsymbol{c}_1^T\boldsymbol{\zeta}_l\right\}\sin(l\pi/L)\\ \mathfrak{Re}\left\{\boldsymbol{c}_2^T\boldsymbol{\zeta}_l\right\}\cos(l\pi/L)+\mathfrak{Im}\left\{\boldsymbol{c}_2^T\boldsymbol{\zeta}_l\right\}\sin(l\pi/L)\\ \vdots\\ \mathfrak{Re}\left\{\boldsymbol{c}_{N_c}^T\boldsymbol{\zeta}_l\right\}\cos(l\pi/L)+\mathfrak{Im}\left\{\boldsymbol{c}_{N_c}^T\boldsymbol{\zeta}_l\right\}\sin(l\pi/L)\end{bmatrix},$$
$$M(l)=\mathfrak{Re}\left\{\boldsymbol{c}_0^T\boldsymbol{\zeta}_l\right\}\cos(l\pi/L)+\mathfrak{Im}\left\{\boldsymbol{c}_0^T\boldsymbol{\zeta}_l\right\}\sin(l\pi/L)-\tau,$$
$$\breve{\boldsymbol{A}}_l=\left[\boldsymbol{A}_1\boldsymbol{\zeta}_l,\boldsymbol{A}_2\boldsymbol{\zeta}_l,\ldots,\boldsymbol{A}_{N_A}\boldsymbol{\zeta}_l\right].$$

Proof: The results follow straightforwardly from Algorithm 2 and using similar steps leading to Theorem 1. □

V. Numerical Results

In this section, we illustrate the effectiveness of our power allocation algorithms for coherent and noncoherent AF relay networks using numerical examples. We determine the RPAs using our proposed algorithms with $\varepsilon=0.001$ and $L=4$ in Sections III and IV.[7] We consider $\boldsymbol{h}_\mathrm{B}$ and $\boldsymbol{h}_\mathrm{F}$ to be mutually independent random vectors with independent and identically distributed elements which are circularly symmetric complex Gaussian r.v.'s, i.e., $h_{\mathrm{B},k}\sim\tilde{\mathcal{N}}(0,1)$ and $h_{\mathrm{F},k}\sim\tilde{\mathcal{N}}(0,1)$ for all k. The noise variances are normalized such that $\sigma_{\mathrm{R},k}^2=1$ and $\sigma_\mathrm{D}^2=1$. For numerical illustrations, we use the outage probability, defined as $\mathbb{P}\{\mathsf{SNR}(\boldsymbol{p})<\gamma_\mathrm{th}\}$, as the performance measure, where γ_th is the value of the target receive SNR and it is set at $\gamma_\mathrm{th}=10$ dB. The uncertainty sets in Theorem 1 is chosen such that $N_A=1$, $N_c=1$, $\boldsymbol{A}_1=\boldsymbol{A}_0$, and $\boldsymbol{c}_1=\boldsymbol{c}_0$. We consider $\rho_1=\rho_2=\rho$, where $\rho=0$ corresponds to perfect knowledge of the global CSI and $\rho=1$ corresponds to an uncertainty that can be as large as the size of the estimated global CSI, i.e., $\boldsymbol{A}_0$ and $\boldsymbol{c}_0$.[8]

Figure 1 shows the outage probability as a function of $P_\mathrm{S}/\sigma_\mathrm{D}^2$ for the coherent AF relay network with $\eta_\mathrm{P}=0.1$. We consider relay networks with $N_\mathrm{r}=10$ and $N_\mathrm{r}=20$, and compare the performance of uniform and optimal RPAs. When $N_\mathrm{r}=10$, both the uniform and optimal power allocations

[7]Our proposed optimal and robust power allocation algorithms, respectively, require solutions of convex feasibility programs in the form of SOCP and SDP. We use the SeDuMi convex optimization package to obtain such numerical solutions[16].

[8]Due to space constraint, we will show the numerical results for the robust RPA for coherent AF relay networks.

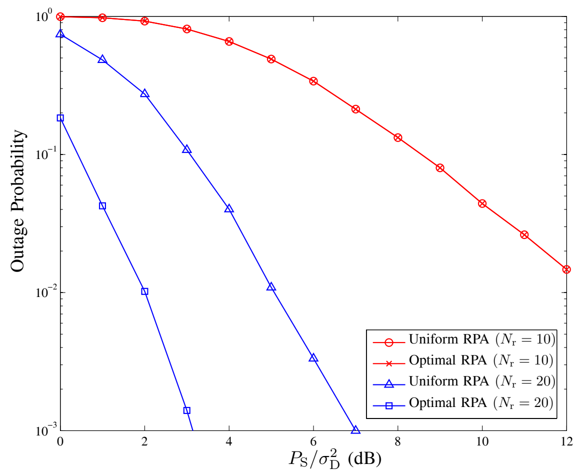

Fig. 1. Outage probability as a function of $P_{\mathrm{S}}/\sigma_{\mathrm{D}}^2$ for the coherent AF relay network with $\eta_{\mathrm{P}} = 0.1$.

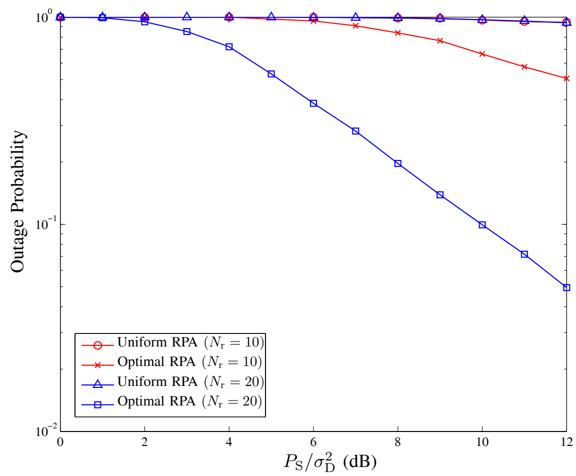

Fig. 2. Outage probability as a function of $P_{\mathrm{S}}/\sigma_{\mathrm{D}}^2$ for the noncoherent AF relay network with $\eta_{\mathrm{P}} = 0.1$.

result in the same performance. This can be explained by the fact that it is optimal for each relay node to transmit at the maximum transmission power P when $\eta_{\mathrm{P}} = P/P_{\mathrm{R}} = 0.1$. When $N_{\mathrm{r}} = 20$, we first observe that lower outage probabilities can be achieved for both power allocations compared to the case with $N_{\mathrm{r}} = 10$, due to the presence of diversity gains in coherent AF relay network. In addition, significant performance improvements with optimal RPA compared to uniform RPA can be observed since optimal RPA can exploit the channel variation more effectively for larger N_{r} to enhance the effective SNR at the destination node.

Similar to Fig. 1, we show the outage probability as a function of $P_{\mathrm{S}}/\sigma_{\mathrm{D}}^2$ for the noncoherent AF relay network with $\eta_{\mathrm{P}} = 0.1$ in Fig. 2. Under uniform RPA, we observe that the increase in the number of relay nodes does not yield any performance gain. This behavior of noncoherent AF relay network is consistent with the results of [17], and can be attributed to the lack of locally-bidirectional CSIs at the relay nodes, making coherent combining at the destination node im-

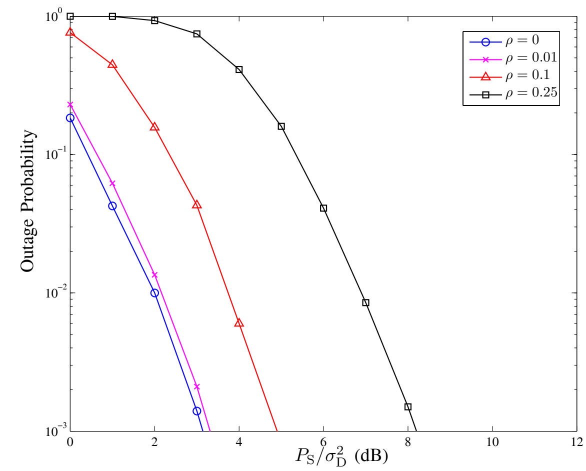

Fig. 3. Effect of uncertain global CSI on the outage probability of the coherent AF relay network using non-robust algorithm for $\eta_{\mathrm{P}} = 0.1$ and $N_{\mathrm{r}} = 20$.

possible. However, we can see that performance improves with optimal RPA compared to uniform RPA, and this improvement increases with N_{r}. Comparing Figs. 1 and 2, even with optimal RPA, the noncoherent AF relay network performs much worse than the coherent AF case, since optimal RPA is unable to fully reap the performance gain promised by coherent AF case due to the lack of distributed beamforming gain.

Figure 3 shows the effect of uncertainties associated with the global CSI on the outage probability of coherent AF networks using non-robust RPAs when $N_{\mathrm{r}} = 20$ and $\eta_{\mathrm{P}} = 0.1$. By non-robust algorithms, we refer to optimization algorithms in Section III that optimize RPAs based only on $\boldsymbol{A}_0$ and $\boldsymbol{c}_0$ instead of the true global CSI $\boldsymbol{A}$ and $\boldsymbol{c}$, where $\boldsymbol{A} = \boldsymbol{A}_0 + z\boldsymbol{A}_1$ and $\boldsymbol{c} = \boldsymbol{c}_0 + u\boldsymbol{c}_1$.[9] Clearly, we see that ignoring CSI uncertainties in our designs can lead to drastic performance degradation when the uncertainty size ρ becomes large. In this figure, we can see that when ρ is less than 0.01, we may ignore CSI uncertainties since the performance degradation is negligible. However, performance deteriorates rapidly as ρ increases.

Figure 4 shows the outage probabilities of coherent AF relay networks as a function of the size of the uncertainty set ρ using robust RPAs when $N_{\mathrm{r}} = 20$ and $\eta_{\mathrm{P}} = 0.1$. For comparison, we also plot the performance of uniform and non-robust RPAs in these plots. We observe that non-robust RPAs still offer some performance improvements over uniform RPAs as long as ρ is not large. When ρ is large, the effectiveness of non-robust RPA algorithms is significantly reduced. On the other hand, we see that robust RPAs provide significant performance gain over non-robust RPAs over a wide range of ρ, showing the effectiveness of our robust algorithms in the presence of global CSI uncertainty.

VI. Conclusion

In this paper, we developed RPA algorithms for coherent and noncoherent AF relay networks. We showed that these

[9] These results are generated based on the worst case scenario, where $z = \rho$ and $u = -\rho$.

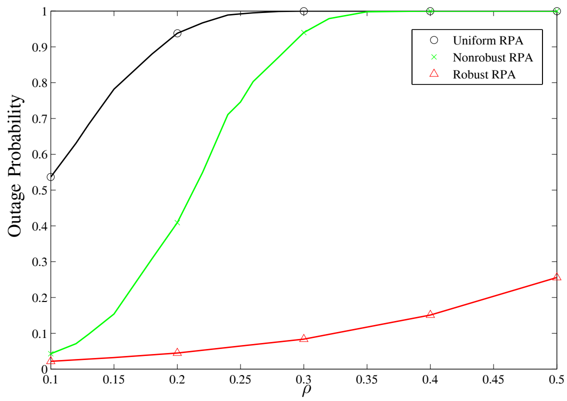

Fig. 4. Outage probability as a function of size of uncertainty set ρ for coherent AF relay network with $P_\mathrm{S}/\sigma_\mathrm{D}^2 = 3$ dB, $\eta_\mathrm{P} = 0.1$, and $N_\mathrm{r} = 20$.

RPA problems, in the presence of perfect global CSI, can be formulated as quasiconvex optimization problems. Thus, the RPA problems can be solved efficiently using the bisection method through a sequence of convex feasibility problems, which can be cast as SOCPs. We developed the robust optimization framework for RPA problems when global CSI is subject to uncertainties. We showed that the robust counterparts of our convex feasibility problems with ellipsoidal uncertainty sets can be formulated as SDPs. Conventionally, uncertainties associated with the global CSI are ignored and the optimization problem is solved as if the given global CSI is perfect. However, our results revealed that such a naive approach often leads to poor performance, highlighting the importance of addressing CSI uncertainties by designing robust algorithms in realistic wireless networks.

Appendix A
Proof of Proposition 1

First, to show that $\mathcal{P}_\mathrm{coh}$ is a quasiconvex optimization problem, we simply need to show that the objective function $f_\mathrm{coh}(\boldsymbol{\zeta})$ is quasiconcave and the constraint set in (10) is convex. The constraint set in (10) is simply the intersection of a hypercube with an SOC. Since the intersection of convex sets is convex, the constraint set in (10) is again convex. For any $t \in \mathbb{R}_+$, the upper-level set of $f_\mathrm{coh}(\boldsymbol{\zeta})$ that belongs to $\mathcal{S}$ is given by

$$\begin{aligned} U(f_\mathrm{coh}, t) &= \left\{ \boldsymbol{\zeta} \in \mathcal{S} : \frac{P_\mathrm{S}}{\sigma_\mathrm{D}^2} \frac{(\boldsymbol{c}^T\boldsymbol{\zeta})^2}{\|\boldsymbol{A}\boldsymbol{\zeta}\|^2+1} \geq t \right\} \\ &= \left\{ \boldsymbol{\zeta} \in \mathcal{S} : \begin{bmatrix} \boldsymbol{c}^T\boldsymbol{\zeta}\sqrt{\frac{P_\mathrm{S}}{t\sigma_\mathrm{D}^2}} \\ \begin{pmatrix} 1 \\ \boldsymbol{A}\boldsymbol{\zeta} \end{pmatrix} \end{bmatrix} \succeq_\mathcal{K} 0 \right\}. \end{aligned} \tag{29}$$

It is clear that $U(f_\mathrm{coh}, t)$ is a convex set since it can be represented as an SOC. Since the upper-level set $U(f_\mathrm{coh}, t)$ is convex for every $t \in \mathbb{R}_+$, $f_\mathrm{coh}(\boldsymbol{\zeta})$ is, thus, quasiconcave. Note that a concave function is also quasiconcave. We now show that $f_\mathrm{coh}(\boldsymbol{\zeta})$ is not concave by contradiction. Suppose that $f_\mathrm{coh}(\boldsymbol{\zeta})$ is concave. We consider $\boldsymbol{\zeta}_a$ and $\boldsymbol{\zeta}_b$ such that $\boldsymbol{\zeta}_a = \zeta_1\boldsymbol{e}_1$ and $\boldsymbol{\zeta}_b = \delta\zeta_1\boldsymbol{e}_1$ for $0 \leq \zeta_1 \leq \sqrt{\eta_\mathrm{P}}$, $\zeta_1^2 \leq 1$, and $0 < \delta < 1$. Clearly, $\boldsymbol{\zeta}_a$ and $\boldsymbol{\zeta}_b \in \mathcal{S}$. For any $\lambda \in [0, 1]$, we have

$$\begin{aligned} f_\mathrm{coh}(\lambda\boldsymbol{\zeta}_a + (1-\lambda)\boldsymbol{\zeta}_b) &= \frac{P_\mathrm{S}/\sigma_\mathrm{D}^2}{\frac{a_1^2}{c_1^2} + \frac{1}{\zeta_1^2[\lambda c_1 + \delta c_1(1-\lambda)]^2}} \\ &\triangleq g(\zeta_1) \end{aligned} \tag{30}$$

where $g(\zeta_1)$ is clearly convex in ζ_1. Due to convexity of $g(\zeta_1)$, the following inequality must hold

$$g(\lambda\zeta_1^{(1)} + (1-\lambda)\zeta_1^{(2)}) \leq \lambda g(\zeta_1^{(1)}) + (1-\lambda) g(\zeta_1^{(2)}). \tag{31}$$

Now, by letting $\zeta_1^{(1)} = \zeta_1/[\lambda + \delta(1-\lambda)]$ and $\zeta_1^{(2)} = \delta\zeta_1/[\lambda + \delta(1-\lambda)]$, we can rewrite (31) as

$$f_\mathrm{coh}(\lambda\boldsymbol{\zeta}_a + (1-\lambda)\boldsymbol{\zeta}_b) \leq \lambda f_\mathrm{coh}(\boldsymbol{\zeta}_a) + (1-\lambda) f_\mathrm{coh}(\boldsymbol{\zeta}_b). \tag{32}$$

Thus, we have showed that there exists $\boldsymbol{\zeta}_a, \boldsymbol{\zeta}_b \in \mathcal{S}$ and $\lambda \in [0, 1]$, such that (32) holds. By contradiction, $f_\mathrm{coh}(\boldsymbol{\zeta})$ is not concave on $\mathcal{S}$.

Appendix B
Proof of Algorithm 1

We first show that for each given t, the convex feasibility program is an SOCP. For each t, the first constraint in (14) follows immediately from (29), which is an SOC constraint. Clearly, the aggregate relay power constraint in (10) can be cast as an SOC constraint. Lastly, the individual relay power constraints can be cast as SOC constraints as follows:

$$\boldsymbol{\zeta}^T\boldsymbol{e}_k \leq \sqrt{\eta_\mathrm{P}} \Leftrightarrow \left\| \begin{pmatrix} \boldsymbol{\zeta}^T\boldsymbol{e}_k \\ \frac{\eta_\mathrm{P}-1}{2} \end{pmatrix} \right\| \leq \frac{\eta_\mathrm{P}+1}{2}. \tag{33}$$

In summary, $\mathcal{P}_\mathrm{coh}^{(\mathrm{SOCP})}$ is an SOCP since $\mathcal{S}_\mathrm{coh}(t)$ is equivalent to the intersection of $(N_\mathrm{r}+2)$ SOC constraints and the objective function is linear.

References

[1] T. Q. S. Quek, H. Shin, and M. Z. Win, “Robust wireless relay networks: slow power allocation with guaranteed QoS," *IEEE J. Sel. Topics Signal Process.*, vol. 1, no. 4, pp. 700-713, Dec. 2007.

[2] A. Ben-Tal and A. Nemirovski, “Robust convex optimization," *Math. Oper. Res.*, vol. 21, no. 4, pp. 769-805, Nov. 1998.

[3] L. E. Ghaoui, F. Oustry, and H. Lebret, “Robust solutions to uncertain semidefinite programs," *SIAM J. Optim.*, vol. 9, no. 1, pp. 33-52, 1998.

[4] M. Gastpar and M. Vetterli, “On the capacity of large Gaussian relay networks," *IEEE Trans. Inf. Theory*, vol. 51, no. 3, pp. 765-779, Mar. 2005.

[5] I. Maric and R. D. Yates, “Bandwidth and power allocation for cooperative strategies in Gaussian relay networks," in *Proc. Asilomar Conf. Signals, Syst. Comput.*, vol. 2, Pacific Grove, CA, Nov. 2004, pp. 1907-1911.

[6] A. Høst-Madsen and J. Zhang, “Capacity bounds and power allocation for wireless relay channels," *IEEE Trans. Inf. Theory*, vol. 51, no. 6, pp. 2020-2040, June 2005.

[7] I. Hammerstrom and A. Wittneben, “On the optimal power allocation for nonregenerative OFDM relay links," in *Proc. IEEE Int. Conf. Commun.*, vol. 10, Istanbul, Turkey, June 2006, pp. 4463-4468.

[8] M. O. Hasna and M.-S. Alouini, “Optimal power allocation for relayed transmissions over Rayleigh-fading channels," *IEEE Trans. Wireless Commun.*, vol. 3, no. 6, pp. 1999-2004, Nov. 2004.

[9] T. Marzetta and B. Hochwald, “Fast transfer of channel state information in wireless systems," *IEEE Trans. Signal Process.*, vol. 54, no. 4, pp. 1268-1278, Apr. 2006.

[10] W. M. Gifford, M. Z. Win, and M. Chiani, “Diversity with practical channel estimation," *IEEE Trans. Wireless Commun.*, vol. 4, no. 4, pp. 1935-1947, July 2005.

[11] T. Q. S. Quek, H. Shin, M. Z. Win, and M. Chiani, "Optimal power allocation for amplify-and-forward relay networks via conic programming," in *Proc. IEEE Int. Conf. Commun.*, Glasgow, Scotland, June 2007, pp. 5058-5063.

[12] ——, "Robust power allocation for amplify-and-forward relay networks," in *Proc. IEEE Int. Conf. Commun.*, Glasgow, Scotland, June 2007, pp. 957-962.

[13] M. S. Lobo, L. Vandenberghe, S. Boyd, and H. Lebret, "Applications of second-order cone programming," *Linear Algebra its Appl.*, vol. 284, pp. 193-228, Nov. 1998.

[14] S. Boyd and L. Vandenberghe, *Convex Optimization*. Cambridge, UK: Cambridge University Press, 2004.

[15] K. Glashoff and K. Roleff, "A new method for chebyshev approximation of complex-valued functions," *Mathematics Computation*, vol. 36, no. 153, pp. 233-239, Jan. 1981.

[16] J. Sturm, "Using SeDuMi 1.02, a MATLAB toolbox for optimization over symmetric cones," *Optim. Meth. Softw.*, vol. 11-12, pp. 625-653, Aug. 1999.

[17] H. Bölcskei, R. Nabar, O. Oyman, and A. Paulraj, "Capacity scaling laws in MIMO relay networks," *IEEE Trans. Wireless Commun.*, vol. 5, no. 6, pp. 1433-1444, June 2006.